**JOURNAL OF ALGEBRAIC STATISTICS**
Volume 13, No. 3, 2022, p. 818 - 837
https://publishoa.com
ISSN: 1309-3452

# Unsteady MHD Slip flow past a inclined porous plate with hall current and temperature gradient dependent heat source with fluctuating temperature and concentration in presence of radiation and Soret effect in a rotating system.

**[1]M.Selvarasu, [2]Dr K.Balamurugan**
[1]Guest lecturer, Department of Mathematics, Thiru A . Govindasamy Government Arts College,Tindivanam 604 307, Tamilnadu ,India,
Email- raasukuty@gmail.com
[2]Associate Professor, Department of Mathematics, Government Arts College,Tiruvannamalai 606 601, Tamilnadu ,India, Email – balamurugankaliyamurthy@yahoo.com

**ABSTRACT**

In this paper, we deal with the analysis of unsteady magnetohydrodynamics slip flow past a heat and mass transfer flow through a non-homogeneous porous medium with variable permeability bounded by an infinite porous inclined plate with hall current and temperature gradient dependent heat source in presence of radiation and soret effect in a rotating system. The flow is considered under the influence of magnetic field applied normal to the flow. Approximate solutions for velocity, temperature and concentration fields are measured using perturbation technique. The expressions for skin-friction rate of heat flux and rate of mass flux are also derived.

**Key words:** MHD, Soret effect, radiation, rotation parameter, chemical reaction, temperature gradient dependent heat source, fluctuating temperature and concentration.

## I.INTRODUCTION

Natural free convection flow induced by buoyancy forces acting over bodies with different geometries in a fluid along a porous medium is prevalent in many natural phenomena and has varied and wide range of industrial applications ,for example in atmospheric flows, the presence of pure air or water is not possible because of some foreign mass many be present naturally or artificially due to industrial emissions. Free convection arises in fluids when temperature changes cause density variation leading to buoyancy forces acting on the fluids elements. Natural processes such as vaporization of mist and fog, photosynthesis are occur due to thermal and buoyancy forces developed as a result of difference in temperature or concentration or a combination of these two. Such configuration plays vital role in industry based applications like heat exchange devices, cooling of molten metals, insulation system, filtration, chemical catalytic reactors and processes.

Hall current is defined as the charge carriers of a current carrying conductor placed in a crosswise magnetic field experience a sideways Lorentz force; this results in a charge separation in a direction vertical to the current and to the magnetic field. The resultant voltage in that direction is proportional to the applied magnetic field. It is frequently used to measure the magnitude of a magnetic field. It is used to find the sign of the dominant charge carriers in materials such as semiconductors. Hall probes are frequently used as magnetometers, i.e. to measure magnetic fields, or inspect materials ( such as tubing or pipeline).

Chemical reactions can be classified as either heterogeneous or homogeneous processes. This depends on whether they occur at an interface or a single phase volume reaction. In well-mixed systems, the reaction is heterogeneous, if it takes place at an interface and homogeneous, if it takes place in solution. In most cases of chemical reaction, the reaction rate depends only on the concentration of the species. A reaction is said to be of first order, if the rate of reaction is directly proportional to the concentration itself.

The theory of rotating fluids has important applications to the motion of fluids on the rotating earth and on the other planets and stars. The atmospheric cyclones illustrate most strikingly the effect of rotation on fluid motion. In such cases, success or failure of the analysis can depend critically on understanding and predicting rotating fluid phenomena oceans and atmosphere are the most visible examples of rotating fluids.

In many practical applications, the particle adjacent to a solid surface no longer takes the velocity of the surface. The particles at the surface has a finite tangential velocities, it slips along the surface. Such a flow regime is called the slip-flow regime and this effect cannot be neglected. At the macroscopic level, it is accepted that the boundary condition for a viscous fluid at a solid wall is the so called no-slip one. While has been proven experimentally to be accurate for a number of macroscopic flows, it remains an assumption that is based on physical principles. In fact nearly two hundred years ago, Navier's proposes a general boundary condition that incorporates the possibility of fluid slip at a solid boundary. Navier's proposed condition assumes that the fluid slip-velocity at a solid surface is proportional to the shear stress at the surface.Agarwal HL et al.[1]have studied that effects of Hall currents on the hydro-magnetic free convection with mass transfer in a rotating fluid. Akindele Michael Okedoye[2] has studied that analytical solution of MHD free convective heat and mass transfer flow in a porous medium. Balamurugan k. et al.[3] have investigated the chemical reaction effects on heat effects on Heat and Mass transfer of unsteady flow over an infinite inclined porous plate embedded in a porous medium with heat source. Balamurugan K.S.et al.[4] have studied the thermo diffusion and chemical reaction effects on a three dimensional MHD mixed convective flow along an infinite vertical porous plate with viscous and joules dissipation.

Jaiswal B.S and Soundalgekar V.M .[5] have studied the oscillating plate temperature effects on a flow past an infinite porous plate with constant suction and embedded in a porous medium. Jha B.K, *et al [6]* have studied mass transfer effects on the flow past an exponentially accelerated vertical plate with constant heat flux. Kim Y.J.[7] has investigated the unsteady MHD Convective heat transfer past a semi-infinite vertical porous moving plate with variable suction.

Kumar H[8] has studied the radiative heat transfer with hydro magnetic flow and viscous dissipation over stretching surface in the presence of variable heat flux. Lighthill M.J.[9] has investigated the response of laminar skin friction and heat transfer to fluctuation in the stream velocity. Makinde O.D.et al.[10] have studied the unsteady free convection flow with suction on an accelerating porous plate. Maygari E.et al.[11] have studied the analytical solutions for unsteady free convection flow through a Porous medium in the stream velocity. Mbeledogu.U and Ogulu.A[12] have investigated that the Heat and mass transfer of an unsteady MHD natural convection flow of a rotating fluid past a vertical porous flat plate in the presence of radiative heat transfer. Muthucumarasamy, R[13] has studied the effect of Heat and mass transfer on flow past an oscillatory vertical plate with variable temperature. Raptis A.A.[14] has investigated the fluid flow through a porous medium in the presence of magnetic field.

## II.FORMULATION OF THE PROBLEM

We consider the flow of an electrically conducting viscous incompressible fluid flow along an infinite inclined porous plate. Choose $x^*$ axis along the plate and $y^*$ axis normal to it. The flow is oriented vertically upward along the $x^*$-direction. Hence all the physical properties of the fluid are functions of $y^*$ and $t^*$. Under the usual Boussinesq approximations the flow is governed by the following system of equations.

$$\frac{\partial v^*}{\partial y^*} = 0$$

(1)

$$\frac{\partial u^*}{\partial t^*} + v^* \frac{\partial u^*}{\partial y^*} + 2K\,w^* = \nu \frac{\partial^2 u^*}{\partial y^{*2}} - \frac{\sigma B_0^{\,2}}{\rho\left(1+m^2\right)}\left(u^* + mw^*\right) + g\beta\left(T^* - T_\infty\right)\cos\alpha + g\beta_c\left(C^* - C_\infty\right)\cos\alpha - \frac{\nu}{K^* p}u^*$$

(2)

$$\frac{\partial w^*}{\partial t^*} + v^* \frac{\partial w^*}{\partial y^*} - 2K\,u^* = \nu \frac{\partial^2 w^*}{\partial y^{*2}} + \frac{\sigma B_0^{\,2}}{\rho\left(1+m^2\right)}\left( mu^* - w^*\right) - \frac{\nu}{K^* p} w^*$$

(3) $$\frac{\partial T^*}{\partial t^*} + v^* \frac{\partial T^*}{\partial y^*} = \frac{k}{\rho C_p}\frac{\partial^2 T^*}{\partial y^{*2}} + \frac{Q^*}{\rho C_p}\frac{\partial T}{\partial y} - \frac{1}{\rho C_p}\frac{\partial q_r^*}{\partial y^*}$$

(4)

$$\frac{\partial C^*}{\partial t^*} + v^* \frac{\partial C^*}{\partial y^*} = D\frac{\partial^2 C^*}{\partial y^{*2}} + \frac{D K_T}{T_M}\frac{\partial^2 T^*}{\partial y^{*2}} - K_o^*\left(C^* - C_\infty^*\right)$$

(5)

The boundary conditions relevant to the problem are;

$$u^* = L_1\left(\frac{\partial u^*}{\partial y^*}\right),\; w^* = L_1\left(\frac{\partial w^*}{\partial y^*}\right), T^* = T_w^* + \varepsilon(T_w^* - T_\infty^*)e^{in^*t^*}$$

$$C^* = C_w^* + \varepsilon(C_w^* - C_\infty^*)e^{in^*t^*} \qquad at\; y^* = 0$$

$$u^* \to 0, T^* \to T_\infty^*, C^* \to C_\infty^* \qquad at\; y^* \to \infty$$

(6)

$u^*, v^*$ and $w^*$ are velocity components of velocity. Along $x^*$-axis, $y^*$-axis and $z^*$-axis directions respectively. g is the acceleration due to gravity, t is the time, $\nu$ is the kinematic viscosity, $\rho$ is the density of the fluid, $\beta$ and $\beta_c$ are the coefficients of volume expansion, $\sigma$ is the electrical conductivity of the fluid, $K_o^*$ is the chemical reaction of the fluid flow, $T^*$ is the temperature, $B_o$ is the uniform magnetic field, $C_p$ is the specific heat at constant pressure, $q_r$ is

JOURNAL OF ALGEBRAIC STATISTICS
Volume 13, No. 3, 2022, p. 818 - 837
https://publishoa.com
ISSN: 1309-3452

the radioactive heat flux, $T_w^*$ is the temperature of the plate, $T_\infty^*$ is the temperature of the fluid away from the plate, $L = \left(\frac{2-m_1}{m_1}\right)$ being the mean free path where $m_1$ is the Maxwell reflection coefficient, $C^*$ is the concentration, $C_w^*$ is the concentration of the fluid at the wall as $C_\infty^*$ is the concentration of the fluid away from the plate.

The equation of continuity (1) yields that $v^*$ is either a constant or some function of time, hence we assume that $v^* = -v_o^*\left(1+\varepsilon e^{-n^*t^*}\right)$

(7)

$v_o^*$ is the suction velocity at the plate and $n^*$ is the positive constant. The negative sign indicates that the suction velocity acts towards the plate.

Consider the fluid which is optically thin with a relatively low density and radioactive heat flux is given by $\frac{\partial q_r^*}{\partial y^*} = 4(T^* - T_\infty^*)I$ ,

(8)

where is the absorption coefficient at the plate.

On introducing the following dimensionless quantities variable

$$y = \frac{y^* v_o^*}{\nu}, t = \frac{v_o^* t^*}{4\nu}, u = \frac{u^*}{v_o^*}, w = \frac{w^*}{v_o^*}, n = \frac{4\nu n^*}{v_o^{*2}}, M = \frac{\sigma B_0^{\,2}\nu}{v_o^{*2}}, Gr = \frac{g\beta\nu(T_w^* - T_\infty^*)}{v_o^{*3}}$$

$$Gm = \frac{g\beta_c\nu(C_w^* - C_\infty^*)}{v_o^{*3}}, Kp = \frac{K^* p v_o^{*2}}{\nu^2}, T = \frac{T^* - T_\infty^*}{T_w^* - T_\infty^*}, C = \frac{C^* - C_\infty^*}{C_w^* - C_\infty^*}, \Pr = \frac{\mu C_p}{k}$$

(9)

$$K = \frac{K^*\nu}{v_o^{*2}}, S_0 = \frac{DK_T\left(T_w^* - T_\infty^*\right)}{\nu T_M\left(C_w^* - C_\infty^*\right)}, K_0 = \frac{K_0'\nu}{v_o^{*2}}, \; R = \frac{4\nu I}{\rho C_p v_o^{*2}}, h = \frac{L_1 v_o^{*2}}{\nu},$$

$$H = \frac{Q^*}{\rho C_p v_o^*}, Sc = \frac{\nu}{D},$$

The equation (2),(3),and (4),(5) becomes

$$\frac{1}{4}\frac{\partial u}{\partial t} - (1+\varepsilon\, e^{-nt})\frac{\partial u}{\partial y} + 2K\, w = \frac{\partial^2 u}{\partial y^2} - \frac{M}{1+m^2}\left(u + mw\right) + GrT\cos\alpha + GmC\cos\alpha - \frac{1}{Kp}u$$

(10)

$$\frac{1}{4}\frac{\partial w}{\partial t} - (1+\varepsilon\, e^{-nt})\frac{\partial w}{\partial y} - 2\,K\,u = \frac{\partial^2 w}{\partial y^2} + \frac{M}{1+m^2}\left(mu - w\right) - \frac{1}{Kp}w$$

(11)

JOURNAL OF ALGEBRAIC STATISTICS
Volume 13, No. 3, 2022, p. 818 - 837
https://publishoa.com
ISSN: 1309-3452

$$\frac{1}{4}\frac{\partial T}{\partial t}-(1+\varepsilon e^{-nt})\frac{\partial T}{\partial y}=\frac{1}{\Pr}\frac{\partial^2 T}{\partial y^2}+H\frac{\partial T}{\partial y}-RT$$

(12)

$$\frac{1}{4}\frac{\partial C}{\partial t}-(1+\varepsilon e^{-nt})\frac{\partial C}{\partial y}=\frac{1}{Sc}\frac{\partial^2 C}{\partial y^2}+S_0\frac{\partial^2 T}{\partial y^2}-K_0 C$$

(13)

The corresponding boundary conditions becomes

$$u=h\frac{\partial u}{\partial y},\ w=h\frac{\partial w}{\partial y},\ T=1+\varepsilon e^{\text{int}},\ C=1+\varepsilon e^{\text{int}},\quad at\ y=0$$

$$u\to 0, T\to 0, C\to 0,\qquad as\ y\to\infty$$

(14)

The equations (10) and (11) can be combined into a single equation by taking $F=u+iw$,we get the following differential equation.

$$\frac{1}{4}\frac{\partial \mathrm{F}}{\partial \mathrm{t}}-(1+\varepsilon\,\mathrm{e}^{-\mathrm{nt}})\frac{\partial \mathrm{F}}{\partial \mathrm{y}}=\frac{\partial^2 \mathrm{F}}{\partial \mathrm{y}^2}-\left(\mathrm{M}_1+\frac{1}{\mathrm{Kp}}-2\mathrm{iK}\right)\mathrm{F}+\mathrm{GrT}\cos\alpha+\mathrm{GmC}\cos\alpha$$

(15)

Where $M_1=\frac{M}{1+m^2}(1-im)$

With boundary conditions,

$$F=h\left(\frac{\partial F}{\partial y}\right)\ ,at\ \ y=0,\qquad F\to 0\,, as\ y\to\infty$$

(16)

## III. METHOD OF SOLUTION

The solve equation (12), (13) and (15), Assuming Ɛ to be small so that one can express F, T and C as a regular perturbation series in terms of Ɛ in the neighborhood of the plate as

$$F(y,t)=F_0(y)+\varepsilon F_1(y)e^{-nt}$$

(17)

$$T(y,t)=T_0(y)+\varepsilon T_1(y)e^{-nt}$$

(18)

$$C(y,t)=C_0(y)+\varepsilon C_1(y)e^{-nt}$$

(19)

**JOURNAL OF ALGEBRAIC STATISTICS**
Volume 13, No. 3, 2022, p. 818 - 837
https://publishoa.com
ISSN: 1309-3452

Using (17),(18),(19) in the equation (12), (13) and (15) equating the coefficient of $\varepsilon^o, \varepsilon'$ neglecting $\varepsilon^2$ terms etc., than we get the set of ordinary differential equations

$$F_0'' + F_0' - \left( M_1 + \frac{1}{Kp} - 2iK \right) F_0 = -Gr\cos\alpha T_0 - Gm\cos\alpha C_0$$

(20)

$$F_1'' + F_1' - \left( M_1 + \frac{1}{Kp} - 2iK - \frac{n}{4} \right) F_1 = -F_0' - Gr\cos\alpha T_1 - Gm\cos\alpha C_1$$

(21)

$$T_0'' + \Pr T_0'(1+H) - R\Pr T_0 = 0$$

(22)

$$T_1'' + \Pr(1+H)T_1' - \left( R - \frac{n}{4} \right) \Pr T_1 = -\Pr T_0'$$

(23)

$$C_0'' + ScC_0' - ScK_0 C_0 = -ScS_0 T_0''$$

(24)

$$C_1'' + ScC_1' - \left( K_0 - \frac{n}{4} \right) ScC_1 = -ScC_0' - ScS_0 T_1''$$

(25)

On solving the above differential equations with following boundary conditions, we get the set of solutions as below

$$F_0 = h\left( \frac{\partial F_0}{\partial y} \right), F_1 = h\left( \frac{\partial F_1}{\partial y} \right), T_0 = 1, T_1 = 1, C_0 = 1, C_1 = 1, \quad y = 0$$

$$F_0 = 0, F_1 = 0, T_0 = 0, T_1 = 0, C_0 = 0, C_1 = 0, \quad y \to \infty$$

$$T_0 = e^{m_1 y}$$

(26)

$$C_0 = A_2 e^{m_2 y} + A_1 e^{m_1 y}$$

(27)

$$F_0 = A_6 e^{m_3 y} + A_3 e^{m_1 y} + A_4 e^{m_2 y} + A_5 e^{m_1 y}$$

(28)

$$T_1 = A_7 e^{m_4 y} + A_8 e^{m_1 y}$$

(29)

$$C_1 = A_9 e^{m_5 y} + A_{10} e^{m_2 y} + A_{11} e^{m_1 y} + A_{12} e^{m_4 y} + A_{13} e^{m_1 y}$$

(30)

**JOURNAL OF ALGEBRAIC STATISTICS**
Volume 13, No. 3, 2022, p. 818 - 837
https://publishoa.com
ISSN: 1309-3452

$$F_1 = A_{14}e^{m_6 y} + A_{15}e^{m_3 y} + A_{16}e^{m_1 y} + A_{17}e^{m_2 y} + A_{18}e^{m_1 y} + A_{19}e^{m_4 y} + A_{20}e^{m_1 y} + A_{21}e^{m_5 y} + A_{22}e^{m_2 y} + A_{23}e^{m_1 y} + A_{24}e^{m_4 y} + A_{25}e^{m_1 y}$$

(31)

The values of the constants $m_1, m_2, m_3, m_4, m_5, m_6, A_1, A_2, A_3, A_4, A_5, A_6, A_7, A_8, A_9, A_{10}, A_{11}, A_{12}, A_{13}, A_{14}, A_{15}, A_{16}, A_{17}, A_{18}, A_{19}, A_{20}, A_{21}, A_{22}, A_{23}, A_{24}, A_{25}$, are given in the Appendix.

3.1. Skin friction

The expression for the skin-friction ( $\tau$ ) at the plate is,

$$\tau = \left(\frac{dF}{dy}\right)_{y=0} = \left(\frac{dF_0}{dy}\right)_{y=0} + \varepsilon\left(\frac{dF_1}{dy}\right)_{y=0} e^{-nt}$$

$$\tau = \left(\frac{dF}{dy}\right)_{y=0} = m_3A_6 + m_1A_3 + m_2A_4 + m_1A_5 + \varepsilon(m_6A_{14} + m_3A_{15} + m_1A_{16} + m_2A_{17} + m_1A_{18} + m_4A_{19} + m_1A_{20} + m_5A_{21} + m_2A_{22} + m_1A_{23} + m_4A_{24} + m_1A_{25})e^{-nt}$$

(32)

3.2. Heat Flux

The rate of heat transfer at the plate of non-dimensional Nusselt number is given by

$$Nu = -\left(\frac{\partial T}{\partial y}\right) = -(m_1 + \varepsilon\left(A_7m_4 + A_8m_1\right)e^{-nt})$$

(33)

3.3. Mass Flux

The rate of mass transfer at the plate of non-dimensional Sherwood Number is given by

$$Sh = -\left(\frac{\partial C}{\partial y}\right)_{y=0} = -(A_2m_2 + A_1m_1 + \varepsilon\left(A_9m_5 + A_{10}m_2 + A_{11}m_1 + A_{12}m_4 + A_{13}m_1\right)e^{-nt})$$

(34)

## IV. RESULTS AND DISCUSSIONS

Here, some of the results of physical interest on the velocity, temperature, concentration distribution and also on the wall shear stress and the rate of heat transfer, rate of mass transfer at the wall were discussed. Further, the result is also in good agreement with the result of Madhusudhana Rao et. al, if omit hall current, soret effect and rotating frame of reference.

We have studied the main flow velocity, temperature and concentration by including various parameters like Prandtl number, suction parameter, Schmidt number, Thermal Grashof number and mass Grashof number.The effect of flow parameteron velocity field, Temperature field, Concentration field, skin friction, heat flux and mass flux have been analyzed numerically and discussed with the help of numerical values.

**JOURNAL OF ALGEBRAIC STATISTICS**
Volume 13, No. 3, 2022, p. 818 - 837
https://publishoa.com
ISSN: 1309-3452

Figure 1 exhibits the effect of the Grashof number (Gr) on the primary velocity distribution. It shows that the primary velocity increases while Gr increases. Gr characterizes the relative effect of the thermal buoyancy force to the viscous hydrodynamic force in the boundary layer flow. Increases in Gr leads to a rise in the velocity owing to the assistance of thermal buoyancy force which induces a favorable pressure gradient. This implies that thermal buoyancy force tends to accelerate velocity. The fluid velocity attains a distinctive maximum value in a region near the surface of the plate and then decays to the free stream value. Figure 2 displays the modified Grashof number (Gm) on the primary velocity distribution. It is observed that the primary velocity increases while Gm increases. Figure 3 displays the hall parameter (m) on the primary velocity distribution. It is observed shows that the primary velocity increases while m increases. Figure 4 display the effect of the Soret number(So) on the primary velocity distribution. It is observed shows that the primary velocity increases while So increases. Figure 5 depicts the effect of the permeability (Kp) on the primary velocity distribution. It is observed shows that the primary velocity increases while Kp increases. Figure 6 reveals the effect of the Slip parameter (h) on the primary velocity distribution. It shows that the primary velocity increases while h increases. Figure 7 depicts the effect of the chemical reaction parameter (Ko) on the primary velocity distribution. It is observed show that the primary velocity increases while Ko decreases. Figure 8 depicts the effect of the radiation parameter (R) on the primary velocity distribution. It is observed show that the primary velocity increases while R decreases. Figure 9 exhibits the effect of the temperature gradient (H) on the primary velocity distribution. It is observed show that the primary velocity increases while H decreases. Figure 10 depicts the effect of the rotating parameter (K) on the primary velocity distribution. It is observed show that the primary velocity increases while K decreases. Figure 11 displays the effect of the prandtl number (Pr) on the primary velocity distribution. It is observed show that the primary velocity increases while Pr decreases. Figure 12 shows the effect of the angle of inclination ($\alpha$) on the primary velocity distribution. It is observed show that the primary velocity increases while $\alpha$ decreases.

Figure 13 depicts the effect of the rotating parameter (K) on the secondary velocity distribution. It is observed show that the secondary velocity increases while K increases. Figure 14 reveals the effect of the Slip parameter (h) on the secondary velocity distribution. It shows that the primary velocity increases while h increases. Figure 15 exhibits the effect of the temperature gradient (H) on the primary velocity distribution. It is observed show that the secondary velocity increases while H decreases.

Figure 16 displays the effect of the temperature gradient (H) on the temperature field . It shows that the temperature decreases while H increases. Figure 17 presents the effect of the radiation parameter (R) on the temperature field . It is observed that the temperature decreases while R increases. Figure 18 displays the effect of the Prandtl number (Pr) on the temperature field . It is noticed that the temperature decreases while Pr increases. It is due to the fact that the thermal boundary layer. The reason is that smaller the values of Pr correspond to larger the thermal conductivity of the field.

The role of played by the Schmidt number, Chemical reaction parameter, Soret number in determining the concentration field is shown in figures 19 to 21. Figure 19 exhibits the effect of the Schmidt number (Sc) on the concentration field. It is observed that the concentration

**JOURNAL OF ALGEBRAIC STATISTICS**
Volume 13, No. 3, 2022, p. 818 - 837
https://publishoa.com
ISSN: 1309-3452

decreases while Sc increases. Figure 20 displays the effect of the chemical reaction parameter (Ko) on the concentration field. It shows that the concentration decreases while Ko increases. Figure 21 demonstrate the effect of the Soret number (So) on the concentration field. It records that the concentration increases while Sc increases.

Figure 22 observed the effect of the Grashof number (Gr) on the skin friction. It is noticed that the skin friction increases while Gr increases. Figuure 23 displays the effect of the Prandtl number (Pr) on the rate of heat flux. It shows that the heat flux increases while Pr increases. Figure 24 depicts the effect of the radiation parameter (R) on the rate of mass flux. It is observed that the mass flux decreases while R increases.

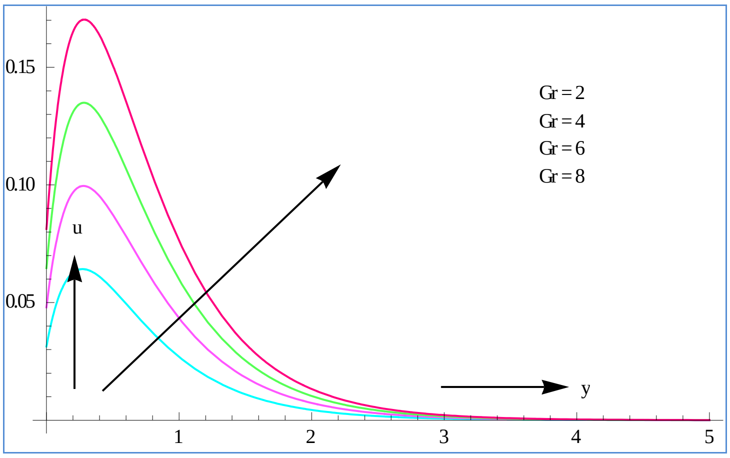


Figure 1: Primary velocity profile for various values of Gr
( Pr = 0.71,H = 1, R = 1, n = 1.0, t = 1.0, $\varepsilon$ = 0.01, Sc = 0.25, Ko = 30, So = 2, M = 3.0, m = 5, K = 0.1, Gm = 2, Kp = 0.1, h = 0.1, cosα = π/6)

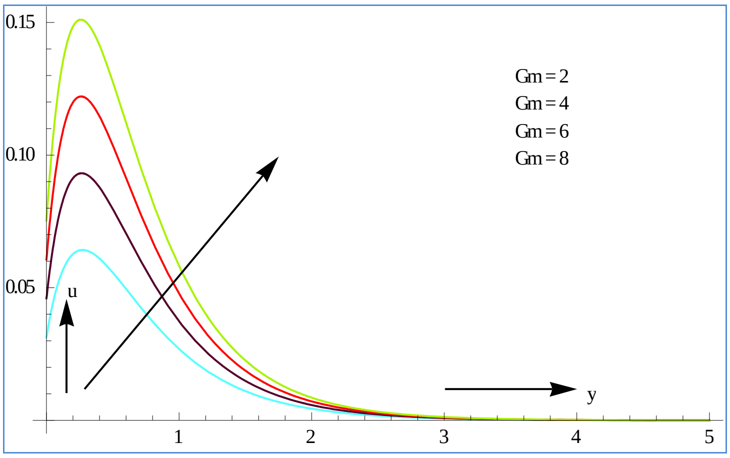


Figure 2: Primary velocity profile for various values of Gm
( Pr = 0.71,H = 1, R = 1, n = 1.0, t = 1.0, $\varepsilon$ = 0.01, Sc = 0.25, Ko = 30, So = 2, M = 3.0, m = 5, K = 0.1, Gr = 2, Kp = 0.1, h = 0.1, cosα = π/6)

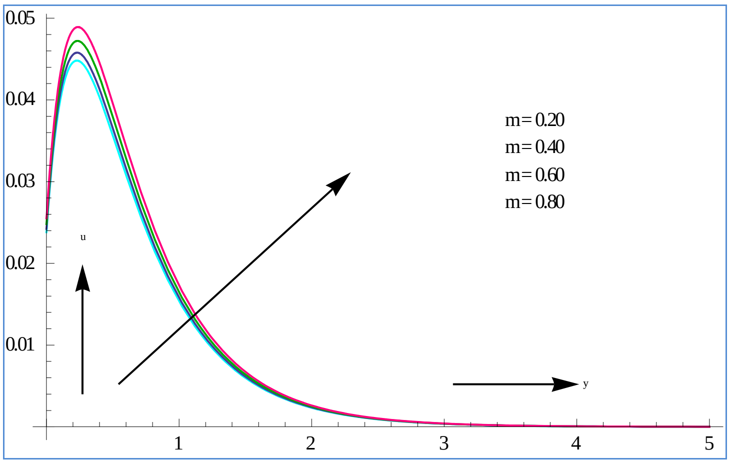


Figure 3: Primary velocity profile for various values of m
( Pr = 0.71,H = 1, R = 1, n = 1.0, t = 1.0, $\varepsilon$ = 0.01, Sc = 0.25, Ko = 30, So = 2, M = 3.0, Gm = 2, K = 0.1, Gr = 2, Kp = 0.1, h = 0.1, cosα = π/6)

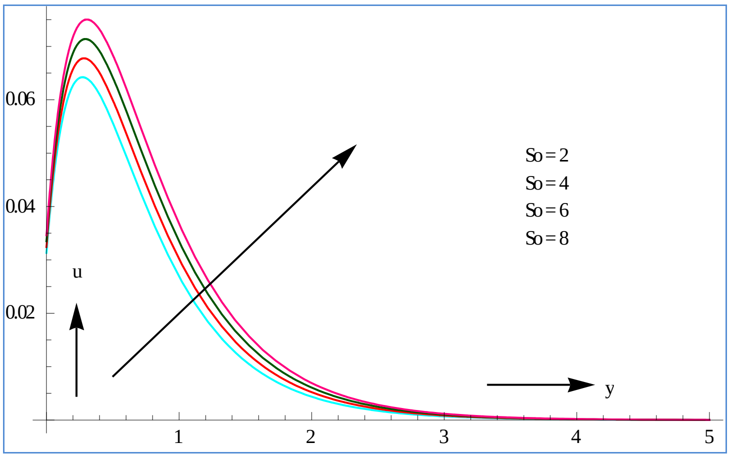


Figure 4: Primary velocity profile for various values of So
( Pr = 0.71,H = 1, R = 1, n = 1.0, t = 1.0, $\varepsilon$ = 0.01, Sc = 0.25, Ko = 30, Gm = 2, M = 3.0, m = 5, K = 0.1, Gr = 2, Kp = 0.1, h = 0.1, cosα = π/6)

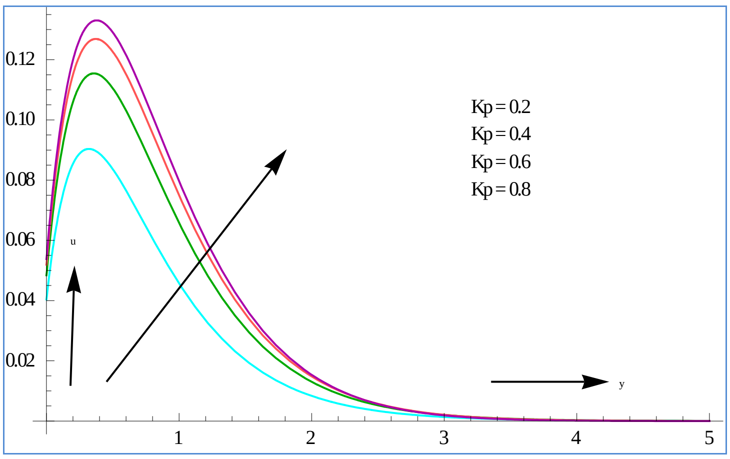


Figure 5: Primary velocity profile for various values of Kp

**JOURNAL OF ALGEBRAIC STATISTICS**
Volume 13, No. 3, 2022, p. 818 - 837
https://publishoa.com
ISSN: 1309-3452

( Pr = 0.71,H = 1, R = 1, n = 1.0, t = 1.0, $\varepsilon$ = 0.01, Sc = 0.25, Ko = 30, So = 2, M = 3.0, m = 5, K = 0.1, Gr = 2, Gm = 2, h = 0.1, cosα = π/6)

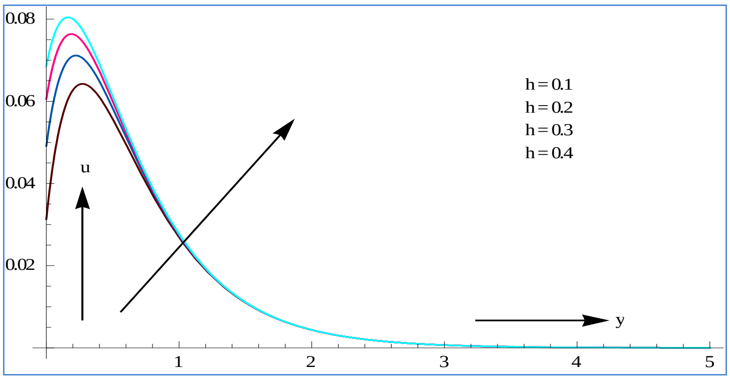


Figure 6: Primary velocity profile for various values of h

( Pr = 0.71,H = 1, R = 1, n = 1.0, t = 1.0, $\varepsilon$ = 0.01, Sc = 0.25, Ko = 30, So = 2, M = 3.0, m = 5, K = 0.1, Gr = 2, Kp = 0.1, Gm = 2, cosα = π/6)

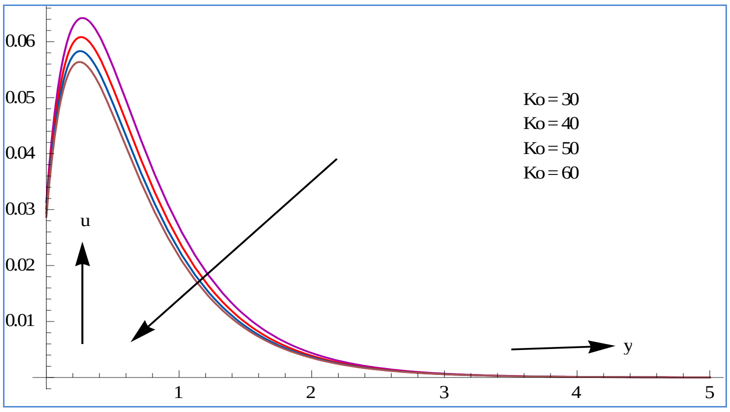


Figure 7: Primary velocity profile for various values of Ko

( Pr = 0.71,H = 1, R = 1, n = 1.0, t = 1.0, $\varepsilon$ = 0.01, Sc = 0.25, Gm = 2, So = 2, M = 3.0, m = 5, K = 0.1, Gr = 2, Kp = 0.1, h = 0.1, cosα = π/6)

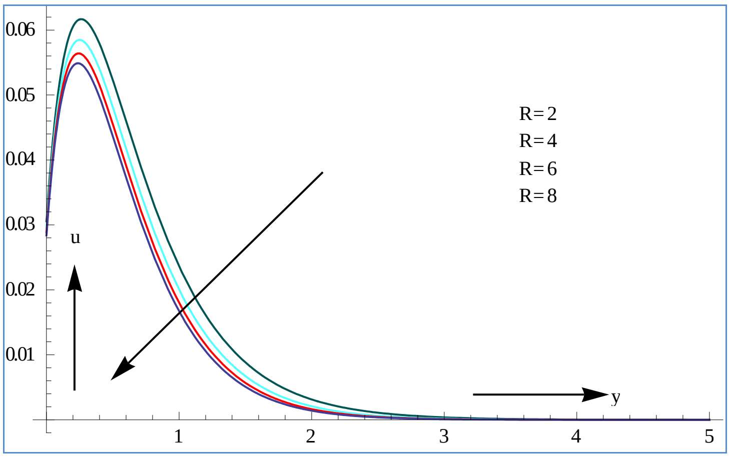


Figure 8: Primary velocity profile for various values of R

( Pr = 0.71,H = 1, Gm = 2, n = 1.0, t = 1.0, $\varepsilon$ = 0.01, Sc = 0.25, Ko = 30, So = 2, M = 3.0, m = 5,

**JOURNAL OF ALGEBRAIC STATISTICS**
Volume 13, No. 3, 2022, p. 818 - 837
https://publishoa.com
ISSN: 1309-3452

K = 0.1, Gr = 2, Kp = 0.1, h = 0.1, cosα = π/6)

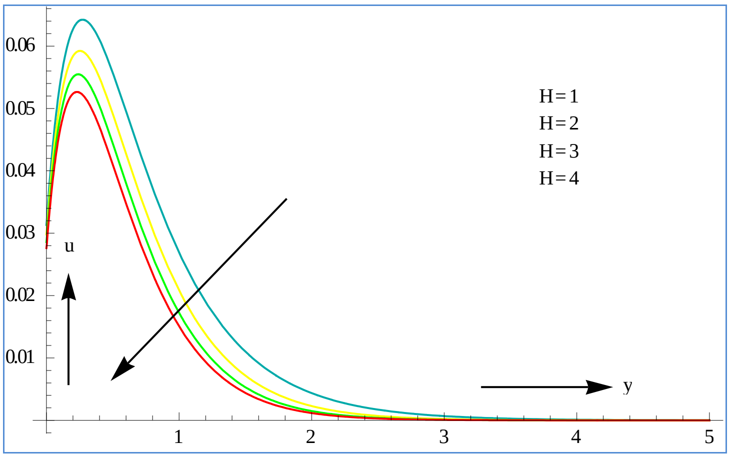


Figure 9: Primary velocity profile for various values of H

( Pr = 0.71,Gm = 2, R = 1, n = 1.0, t = 1.0, $\varepsilon$ = 0.01, Sc = 0.25, Ko = 30, So = 2, M = 3.0, m = 5, K = 0.1, Gr = 2, Kp = 0.1, h = 0.1, cosα = π/6)

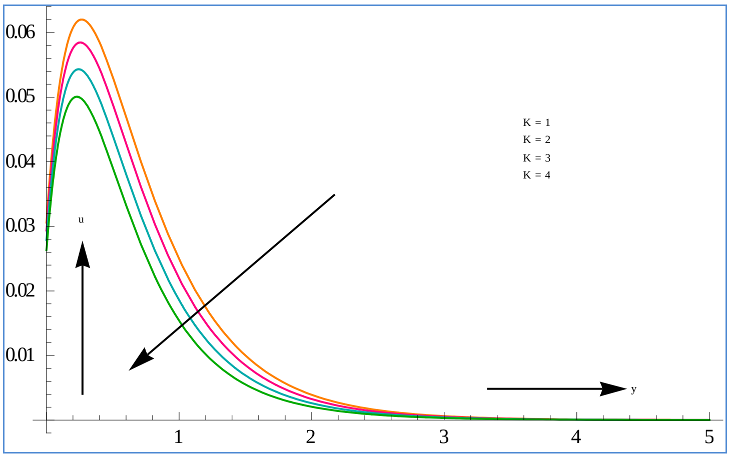


Figure 10: Primary velocity profile for various values of K

( Pr = 0.71,Gm = 2, R = 1, n = 1.0, t = 1.0, $\varepsilon$ = 0.01, Sc = 0.25, Ko = 30, So = 2, M = 3.0, m = 5, H =1, Gr = 2, Kp = 0.1, h = 0.1, cosα = π/6)

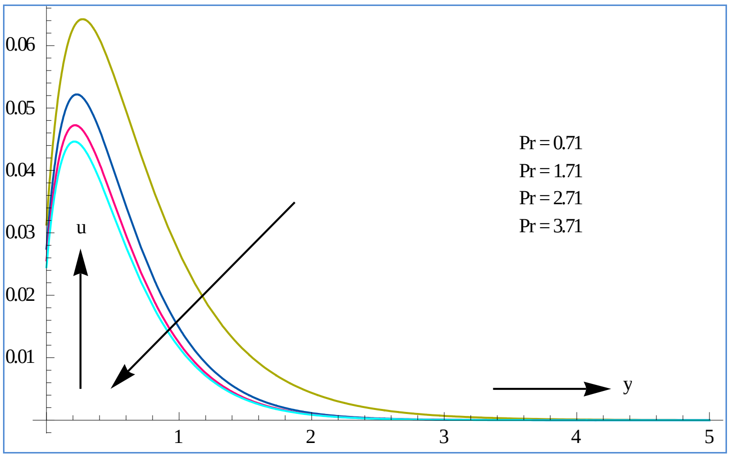


Figure 11: Primary velocity profile for various values of Pr

**JOURNAL OF ALGEBRAIC STATISTICS**
Volume 13, No. 3, 2022, p. 818 - 837
https://publishoa.com
ISSN: 1309-3452

( H = 1, R = 1, n = 1.0, t = 1.0, $\varepsilon$ = 0.01, Sc = 0.25, Ko = 30, So = 2, M = 3.0, m = 5, Gm = 2, K = 0.1, Gr = 2, Kp = 0.1, h = 0.1, cosα = π/6)

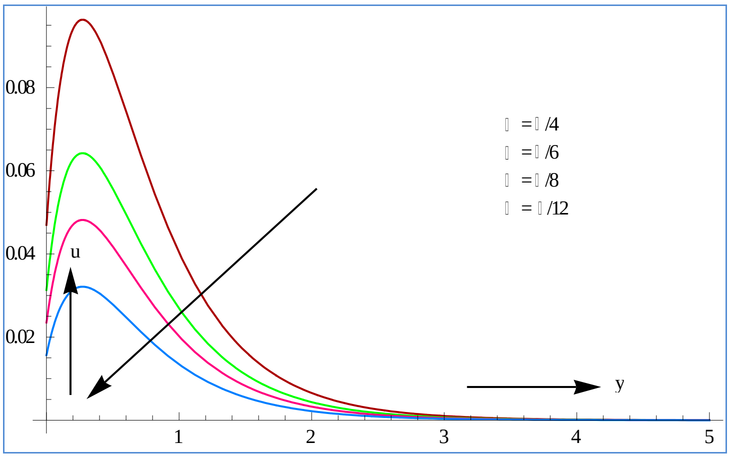


Figure 12: Primary velocity profile for various values of α

( Pr = 0.71,H = 1, R = 1, n = 1.0, t = 1.0, $\varepsilon$ = 0.01, Sc = 0.25, Ko = 30, So = 2, M = 3.0, m = 5, K = 0.1, Gr = 2, Kp = 0.1, h = 0.1, Gm = 2)

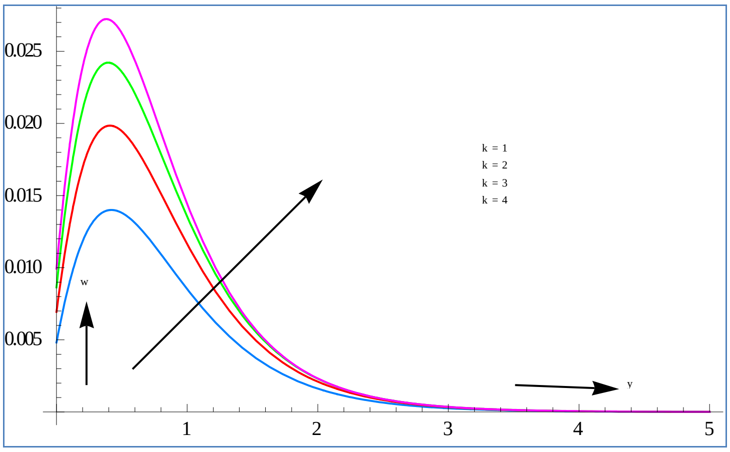


Figure 13: Secondary velocity profile for various values of K

( Pr = 0.71,H = 1, R = 1, n = 1.0, t = 1.0, $\varepsilon$ = 0.01, Sc = 0.25, Ko = 30, So = 2, M = 3.0, m = 5, Cos α = π/6, Gr = 2, Kp = 0.1, h = 0.1, Gm = 2)

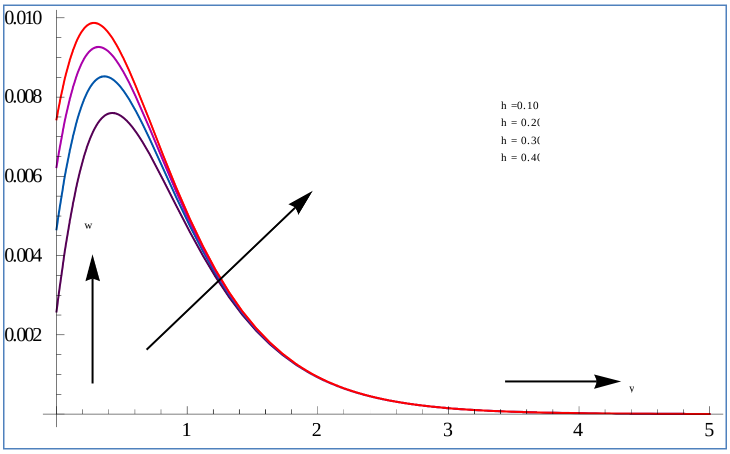


Figure 14: Secondary velocity profile for various values of h

**JOURNAL OF ALGEBRAIC STATISTICS**
Volume 13, No. 3, 2022, p. 818 - 837
https://publishoa.com
ISSN: 1309-3452

( Pr = 0.71,H = 1, R = 1, n = 1.0, t = 1.0, $\varepsilon$ = 0.01, Sc = 0.25, Ko = 30, So = 2, M = 3.0, m = 5, Cos α = π/6, Gr = 2, Kp = 0.1, K = 0.1, Gm = 2)

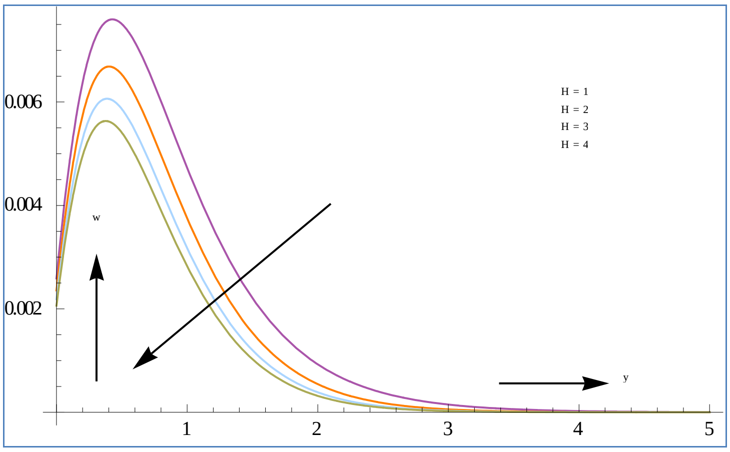


Figure 15: Secondary velocity profile for various values of H

( Pr = 0.71,K = 0.1, R = 1, n = 1.0, t = 1.0, $\varepsilon$ = 0.01, Sc = 0.25, Ko = 30, So = 2, M = 3.0, m = 5, Cos α = π/6, Gr = 2, Kp = 0.1, h = 0.1, Gm = 2)

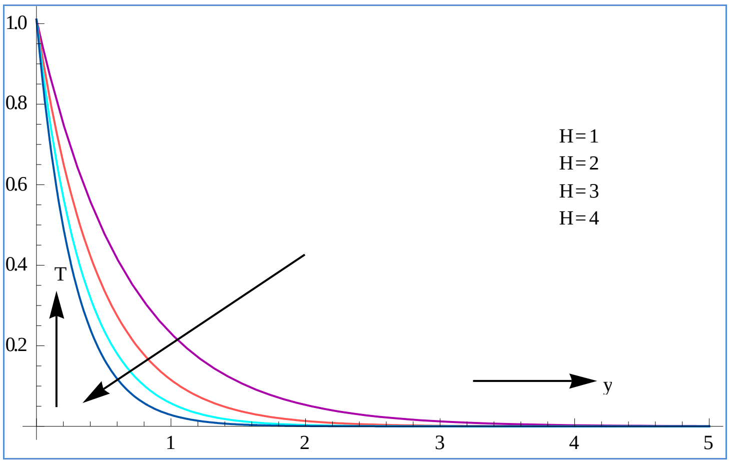


Figure 16: Temperature profile for various values of H

( Pr = 0.71, R = 1, n = 1.0, t = 1.0, $\varepsilon$ = 0.01)

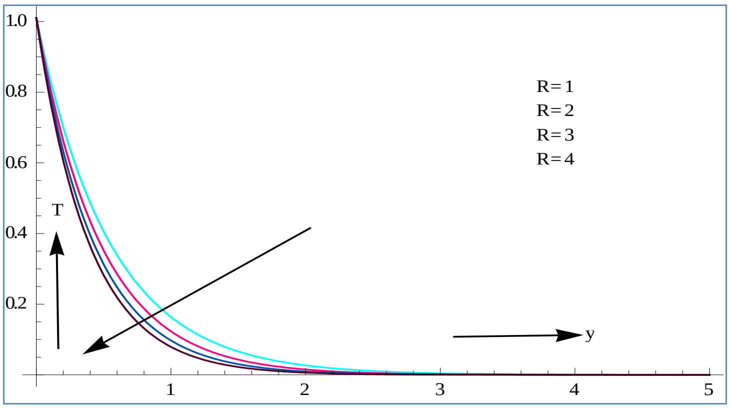


Figure 17: Temperature profile for various values of R

**JOURNAL OF ALGEBRAIC STATISTICS**
Volume 13, No. 3, 2022, p. 818 - 837
https://publishoa.com
ISSN: 1309-3452

( Pr = 0.71, H = 1, n = 1.0, t = 1.0, $\varepsilon$ = 0.01)

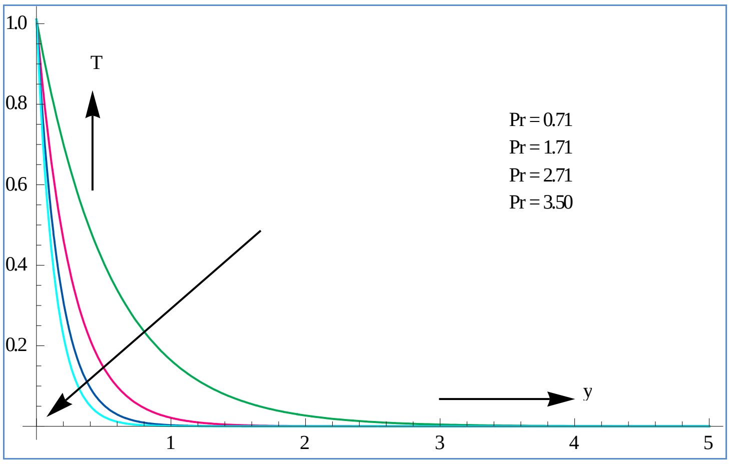


Figure 18: Temperature profile for various values of Pr

( H = 1, R = 1, n = 1.0, t = 1.0, $\varepsilon$ = 0.01)

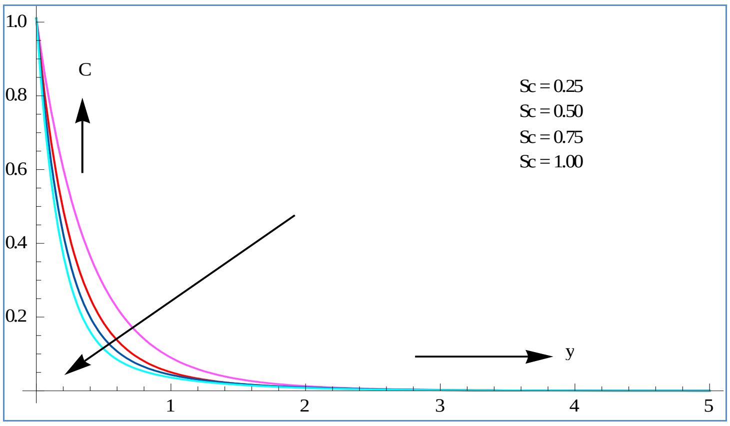


Figure 19: Concentration profile for various values of Sc

( Pr = 0.71,H = 1, R = 0.1, n = 1.0, t = 1.0, $\varepsilon$ = 0.01, Gm = 2, Ko = 30, So = 2, M = 3.0, m = 5, K = 0.1, Gr = 2, Kp = 0.1, h = 0.1, cosα = π/6)

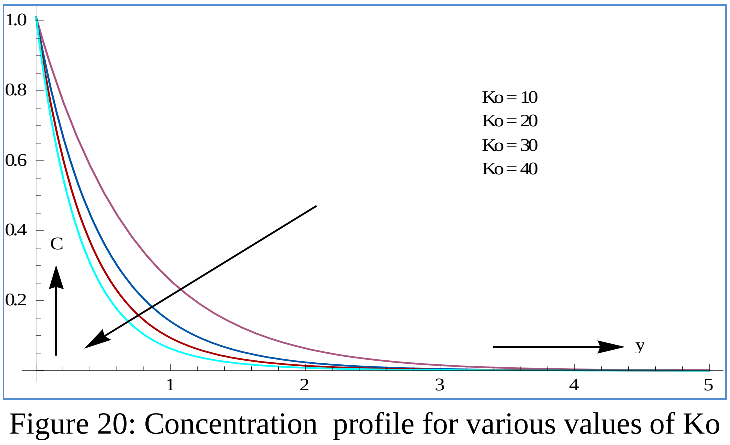


Figure 20: Concentration profile for various values of Ko

( Pr = 0.71,H = 1, R = 0.1, n = 1.0, t = 1.0, $\varepsilon$ = 0.01, Gm = 2, Sc = 0.25, So = 2, M = 3.0, m = 5, K = 0.1, Gr = 2, Kp = 0.1, h = 0.1, cosα = π/6)

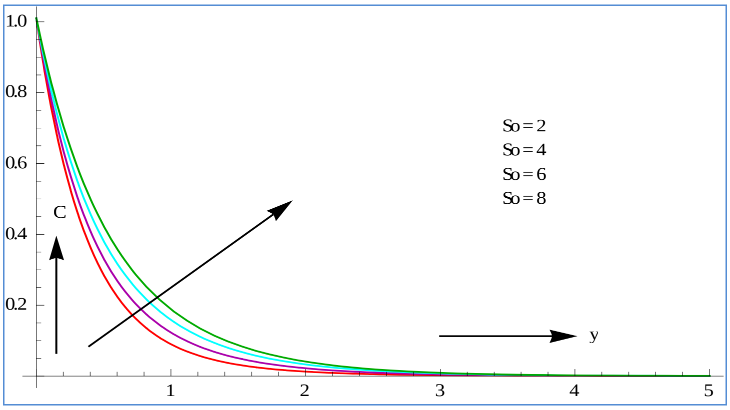


Figure 21: Concentration profile for various values of So

( Pr = 0.71,H = 1, R =0. 1, n = 1.0, t = 1.0, $\varepsilon$ = 0.01, Gm = 2, Ko = 30, Sc = 0.25, M = 3.0, m = 5,
K = 0.1, Gr = 2, Kp = 0.1, h = 0.1, cosα = π/6)

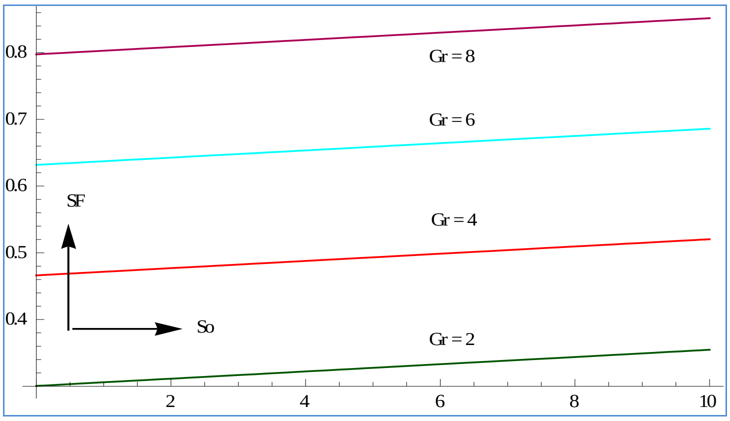


Figure 22: Skin friction for various values of Gr

( Pr = 0.71,H = 1, R = 1, n = 1.0, t = 1.0, $\varepsilon$ = 0.01, Sc = 30, Ko = 30, So = 2, M = 3.0, m = 5,
K = 0.1, Gm = 2, Kp = 0.1, h = 0.1, cosα = π/6)

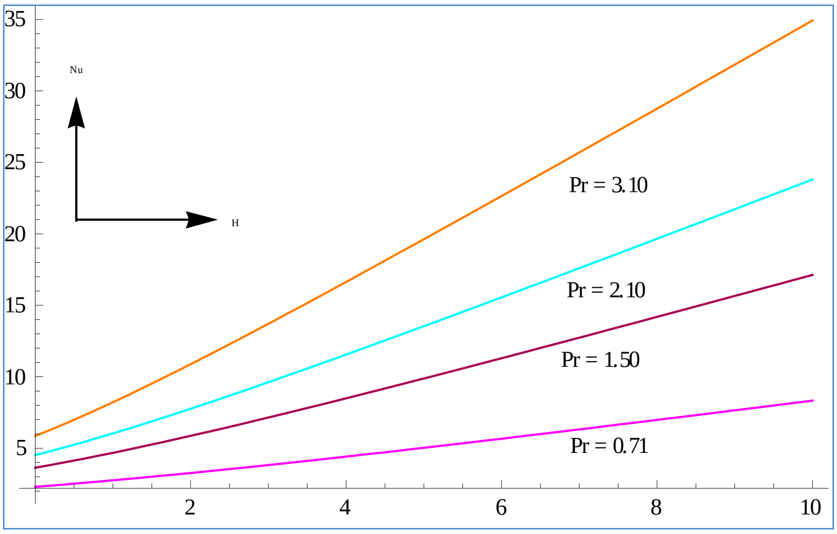


Figure 23: Heat flux for various values of H

( H = 1, R = 1, n = 1.0, t = 1.0, $\varepsilon$ = 0.01)

**JOURNAL OF ALGEBRAIC STATISTICS**
Volume 13, No. 3, 2022, p. 818 - 837
https://publishoa.com
ISSN: 1309-3452

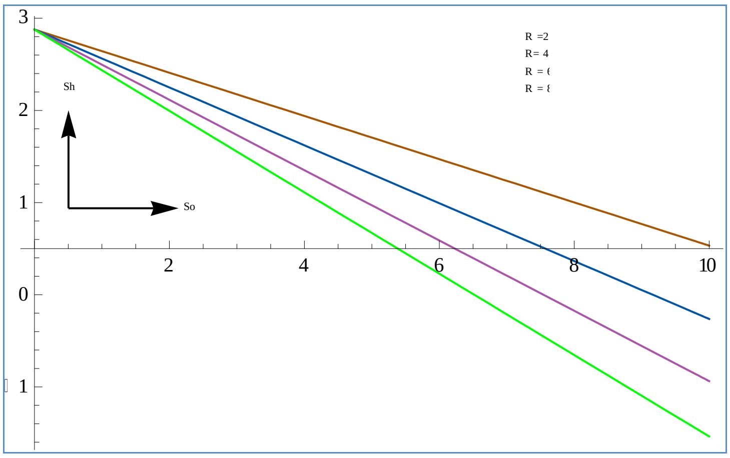


Figure 24: Mass flux for various values of R
( Pr = 0.71,H = 1, Sc = 0.25, n = 1.0, t = 1.0, $\varepsilon$ = 0.01, Gm = 2, Ko = 30, So = 2, M = 3.0, m = 5, K = 0.1, Gr = 2, Kp = 0.1, h = 0.1, cosα = π/6)

## V. CONCLUSIONS

In this work, we have studied the Hall effects on magnetohydrodynamics slip flow past a porous vertical plate with radiation and Soret effect in rotating system.The governing equations are solved by using perturbation techniques. An asymptotic solution of the resulting differential equations under the prescribed boundary conditions is obtained. Numerical results are discussed with help of graphs. The conclusions of the study are as follows:

- Primary velocity increases with the increase in the Grashof number, Modified Grashof number, Hall parameter, Soret number, permeability and Slip parameter; whereas it retards with the increase in the Chemical reaction, Radiation parameter, Temperature gradient, Prandtl number, angle of inclination,
- secondary velocities increase with the increase in the Rotating parameter and Slip parameter. Increase of Soret effect enhances the velocity of the fluid flow. Increase of temperature gradient decreases the secondary velocity.
- Temperature decreases with the increase in Temperature gradient, Radiation parameter, and Prandtl number.
- Concentration increases with the increase in to Soret number; whereas it retards with the increase in Schmidt number, Chemical reaction parameter.
- Skin friction increases with the increase in Grashof number.
- Heat flux shows the increased effect if increase of Prandtl number and mass flux shows the decreased effect while increase of radiation parameter.

## REFERENCE

1. H.L. Agarwal, P.C. Ram and V. Singh, Effects of Hall currents on the hydro- magnetic free convection with mass transfer in a rotating fluid. Astrophys space science, 1984,100,279-283.

2. Akindele Michael Okedoye, Analytical solution of MHD free convective heat and mass Transfer flow in a porous medium".The Pacific Journal of Science and Technology, 2013,14,2, 225-245
3. K. Balamurugan, S. Anuradha and R. Karthikeyan, Chemical reaction effects on Heat and Mass Transfer of Unsteady flow over an infinite vertical porous plate embedded in a porous medium with heat source". International Journal of Scientific and Engineering Research, 2014,5, ,1179-1193
4. K.S. Balamurugan, S.V.K. Varma, K. Ramakrishanaprasad, Thermo diffusion and chemicalreaction effects on a three dimensional MHD Mixed convective flow along an infinite vertical porous plate with viscous and Joules dissipation. International Journal of Advances in Science and Technology.2001.3, 73-92.
5. Jaiswal B.S and Soundalgekar V.M., Oscillating plate temperature effects on a flow past an infinite porous plate with constant suction and embedded in a porous medium. Heat and Energy.1986,10,97-100
6. B.S. Jha, R. Prasad and S. Rai, Mass Transfer effects on the flow past an exponentially Accelerated vertical plate with constant heat flux. Astrophysics and space science, 1991,181, 125-134.
7. Y.J. Kim, Unsteady MHD Convective heat transfer past a semi-infinite vertical porous Moving plate with variable suction. International Journal of EngineeringScience.2000, 38,833-845.
8. H.Kumar, Radiative heat transfer with hydro magnetic flow and viscous dissipation over stretching surface in the presence of variable heat flux. Thermal Science, 2009, 13, 163-169.
9. M.J. Lighthill, The response of laminar skin friction and heat transfer to fluctuation in the in the stream velocity.Proc.R.Soc.A, 1954,224, 1-23.
10. O.D. Makinde, J.M. Mango, D.M. Theuri. Unsteady free convection flow with suction on an Accelerating porous plate.AMSE.J.Mod.Meas.2003, 72, 39-46.
11. E. Maygari, I.Pop and B. Keller. "Analytical solutions for Unsteady free convection flow through a Porous media" .Journal of Engineering Math.2004,48,93-104
12. U. Mbeledogu and A.Ogulu. Heat and mass transfer of an unsteady MHD natural convection flow of a rotating fluid past a vertical porous flat plate in the presence of radiative heat transfer. International Journal of Heat and Mass Transfer.2007, 1902-1908.13.
13. R. Muthucumarasamy, Effect of Heat and mass transfer on flow past an oscillatory vertical plate with variable temperature. International Journal of Appl.Math and Mech, 2008, 4, 59-65.
14. A.A. Raptis, Flow through a porous medium in the presence of magnetic field. International Journal of International Journal of Energy.1986, 10, 97-100.
15. A.A. Raptis, N. Kafousias, "Heat Transfer in flow through a porous medium bounded by an infinite vertical plate under the action of a magnetic field". Int.J.Energy .1982, 6,241-245.
16. K. Sarada and B. Shanker, 2013, "The Effects of Soret and Dufour on an unsteady MHD free Convection flow past a vertical porous plate in the presence of suction or injection". International Journal of Engineering and Science, 2013, 2, 7, 35-46.
17. K.D. Singh and R. Kumar, 2009, "Combine effects of hall current and rotation on free convection MHD flow in a porous channel". Indian Journal of Pure and Applied Physics,2009, 47,617-623

18. G. Srinivasa Rao *et.al*. Soret and Dufour effects on MHD Boundary layer flow over amoving vertical porous plate with suction".International Journal of Emerging Trends in Engineering and Development, 2014,4, 2, 63-72

## APPENDIX

$$m_1 = \frac{-\Pr(1+H) - \sqrt{\Pr^2(1+H)^2 + 4\Pr R}}{2}, m_2 = \frac{-Sc - \sqrt{Sc^2 + 4ScKo}}{2}$$

$$m_3 = \frac{-1 - \sqrt{1 + 4(\frac{1}{Kp} + M1 - 2iK)}}{2}, \quad m_4 = \frac{-\Pr(1+H) - \sqrt{\Pr^2(1+H)^2 + 4\Pr(R - \frac{n}{4})}}{2}, \quad m_5 = \frac{-Sc - \sqrt{Sc^2 + 4(Ko - \frac{n}{4})Sc}}{2},$$

$$m_6 = \frac{-1 - \sqrt{1 + 4(\frac{1}{Kp} + M1 - 2iK - \frac{n}{4})}}{2},$$

$$A_1 = \frac{-ScSom_1^2}{m_1^2 + Sc\, m_1 - ScKo}, A_2 = 1 - A_1;$$

$$A_3 = \frac{-Gr\cos\alpha}{m_1^2 + m_1 - (M_1 + \frac{1}{Kp} - 2iK)}, A_4 = \frac{-A_2 Gm\cos\alpha}{m_2^2 + m_2 - (M_1 + \frac{1}{Kp} - 2iK)}, A_5 = \frac{-A_1 Gm\cos\alpha}{m_1^2 + m_1 - (M_1 + \frac{1}{Kp} - 2iK)},$$

$$A_6 = \frac{-1}{(1-hm_3)}(A_3(1-hm_1) + A_4(1-hm_2) + A_5(1-hm_1)), A_7 = 1 - A_8, A_8 = \frac{-\Pr m_1}{m_1^2 + (1+H)\Pr m_1 - (R - \frac{n}{4})\Pr},$$

$$A_9 = 1 - \left(A_{10} + A_{11} + A_{12} + A_{13}\right), A_{10} = \frac{\left(-Sc\, m_2\, A_2\right)}{m_2^2 + Sc\, m_2 - Sc\left(Ko - \frac{n}{4}\right)}$$

$$A_{11} = \frac{\left(-Sc\, m_1\, A_1\right)}{m_1^2 + Sc\, m_1 - Sc\left(Ko - \frac{n}{4}\right)}, A_{12} = \frac{\left(-ScSo\, m_4^2\, A_7\right)}{m_4^2 + Sc\, m_4 - Sc\left(Ko - \frac{n}{4}\right)},$$

$$A_{13} = \frac{\left(-ScSo\, m_1^2\, A_8\right)}{m_1^2 + Sc\, m_1 - Sc\left(Ko - \frac{n}{4}\right)},$$

$$A_{14} = -\frac{1}{(1-hm_6)}\begin{pmatrix} A_{15}\ (1-h\,m_3) + A_{16}\ (1-h\,m_1) + A_{17}\ (1-h\,m_2) \\ + A_{18}\ (1-h\,m_1) + A_{19}\ (1-h\,\mathrm{m}_4) + A_{20}\ (1-h\,m_1) \\ + A_{21}\ (1-h\,m_5) + A_{22}\ (1-h\,m_2) + A_{23}\ (1-h\,m_1) \\ + A_{24}\ (1-h\,m_4) + A_{25}\ (1-h\,m_1) \end{pmatrix}$$

**JOURNAL OF ALGEBRAIC STATISTICS**
Volume 13, No. 3, 2022, p. 818 - 837
https://publishoa.com
ISSN: 1309-3452

$$A_{15} = \frac{-m_3 A_6}{m_3^{\,2} + m_3 - (M_1 + \frac{1}{Kp} - 2iK - \frac{n}{4})}, A_{16} = \frac{-m_1 A_3}{m_1^{\,2} + m_1 - (M_1 + \frac{1}{Kp} - 2iK - \frac{n}{4})},$$

$$A_{17} = \frac{-m_2 A_4}{m_2^{\,2} + m_2 - (M_1 + \frac{1}{Kp} - 2iK - \frac{n}{4})}, A_{18} = \frac{-m_1 A_5}{m_1^{\,2} + m_1 - (M_1 + \frac{1}{Kp} - 2iK - \frac{n}{4})},$$

$$A_{19} = \frac{-Gr \cos\alpha A_7}{m_4^{\,2} + m_4 - (M_1 + \frac{1}{Kp} - 2iK - \frac{n}{4})}, A_{20} = \frac{-Gr \cos\alpha A_8}{m_1^{\,2} + m_1 - (M_1 + \frac{1}{Kp} - 2iK - \frac{n}{4})},$$

$$A_{21} = \frac{-Gm \cos\alpha A_9}{m_5^{\,2} + m_5 - (M_1 + \frac{1}{Kp} - 2iK - \frac{n}{4})}, A_{22} = \frac{-Gm \cos\alpha A_{10}}{m_2^{\,2} + m_2 - (M_1 + \frac{1}{Kp} - 2iK - \frac{n}{4})},$$

$$A_{23} = \frac{-Gm \cos\alpha A_{11}}{m_1^{\,2} + m_1 - (M_1 + \frac{1}{Kp} - 2iK - \frac{n}{4})}, A_{24} = \frac{-Gm \cos\alpha A_{12}}{m_4^{\,2} + m_4 - (M_1 + \frac{1}{Kp} - 2iK - \frac{n}{4})},$$

$$A_{25} = \frac{-Gm \cos\alpha A_{13}}{m_1^{\,2} + m_1 - (M_1 + \frac{1}{Kp} - 2iK - \frac{n}{4})},$$